

**The Influence of Opacity on
Hydrogen Line Emission and Ionisation Balance
in High Density Divertor Plasmas**

K. Behringer

IPP 10/5

February 1997



MAX-PLANCK-INSTITUT FÜR PLASMAPHYSIK

85748 GARCHING BEI MÜNCHEN

MAX-PLANCK-INSTITUT FÜR PLASMAPHYSIK
GARCHING BEI MÜNCHEN

The Influence of Opacity on
Hydrogen Line Emission and Ionisation Balance
in High Density Divertor Plasmas

K. Behringer

IPP 10/5

February 1997

*Die nachstehende Arbeit wurde im Rahmen des Vertrages zwischen dem
Max-Planck-Institut für Plasmaphysik und der Europäischen Atomgemeinschaft über
die Zusammenarbeit auf dem Gebiete der Plasmaphysik durchgeführt.*

Abstract

The ADAS208 collisional-radiative model was employed to calculate excitation, ionisation and recombination coefficients for hydrogen atoms and optically thin, as well as optically thick plasma conditions. The required input data were drawn from the relevant specific ion files in the ADAS data base. The optical thickness of resonance lines was taken into account by reducing the optically thin transition probabilities, i.e. by multiplying them by an escape factor $\Theta \leq 1$. Escape factors for ASDEX Upgrade density limit plasma conditions were calculated by means of a PC program on the basis of some simplifying assumptions. The calculated ionisation and recombination rate coefficients demonstrate the processes of stepwise ionisation and recombination into excited levels, which are a function of the optical thickness of the Lyman lines. They were used to calculate the equilibrium ionisation balance and the recombination contribution to excited level population, and are also available for plasma simulation codes. In the electron density range between 10^{12} and 10^{17} cm^{-3} the excited states show the transition from Corona to Boltzmann equilibrium, which occurs earlier in cases of optically thickness. A comparison of the results for the optically thin and thick cases demonstrates that the opacity of (essentially) L_α leads to an increase in ionisation degree of almost an order of magnitude and to a similar enhancement in hydrogen line radiation for the relevant plasma conditions. Above $n_e \approx 10^{14} \text{ cm}^{-3}$ the hydrogen excited states with principal quantum numbers n greater than 2 are close to Saha equilibrium with electrons and ions (PLTE), if the neutral density is not far from the atomic physics equilibrium value. This allows a T_e analysis by means of a Boltzmann plot and an approximate calculation of the ionisation balance without explicitly using the ionisation and recombination coefficients. The excitation and recombination coefficients calculated by ADAS208 were analysed to separate the two contributions to spectral line emission for ionisation degrees far from equilibrium. If the ground state excitation is significant, the plasma neutral density can be measured from the Balmer spectral line emission. However, the electron temperature must be known precisely for this procedure, and most likely the neutral density cannot be determined in this way in the ASDEX Upgrade divertor and for density limit conditions, because it is too low. These plasmas are probably characterised by volume recombination, but recombination only plays a role as a particle sink if the flow velocities are substantially below sound speed.

This is the first IPP report on ADAS applications for fusion which will be followed by papers on the calculation of diagnostic line data, of total line radiation and of ionisation and recombination coefficients for various elements

Introduction

In cold, dense divertor plasmas, as e.g. realised in ASDEX Upgrade density limit discharges, recombination of hydrogen ions with density n_i may become an important process and may result in high densities of neutral hydrogen atoms n_0 . The ionisation degree, i.e. n_i/n_0 , possibly falls to very low values of a few per cent. Under these conditions it is very likely that the hydrogen resonance lines (Lyman lines) are optically thick for the relevant plasma geometry. This opacity effect changes the population of excited states with densities n_k and also the effective collisional-radiative ionisation and recombination rate coefficients S and α . In this situation, atomic data for excitation and ionisation are required, which take into account the consequence of optical thickness of the Lyman and possibly also the Balmer lines. In atomic physics codes opacity effects can be introduced by reducing the transition probabilities A of the resonance lines, i.e. by multiplying them by a so-called escape factor $\Theta \leq 1$ [1]. In the present study an attempt was made to calculate the increase in hydrogen line emission and the change in ionisation balance due to optical thickness. The basic atomic data were taken from the JET / Strathclyde Atomic Data Analysis Structure ADAS [2], and some ADAS atomic physics codes were used. However, a few extra programs, usually written for the PC and in BASIC language, were also required for the described analysis. Some other applications of the ADAS system are being mentioned in the following discussion of the results.

The Collisional-Radiative Code ADAS208

ADAS208 computes the collisional-radiative excited state population of atoms and ions on the basis of the specific ion files stored under ADAS directory *adf04*. These specific ion files are normally also provided by the central data base. In their minimum configuration, they contain energy levels, transition probabilities and electron impact excitation rate coefficients. They may also have information on radiative recombination, on charge exchange and on proton collisions in lines which are marked correspondingly. Ionisation out of ground and metastable states, as well as that of excited states can be included according to standard formulae. It is also possible to use more up-to-date ionisation rate coefficients from ADAS group *adf07* (*szd<yr>#<el>_<el>.dat*, see below for an explanation of the annotation) by means of the "ionisation coefficient search" option calling in the ADAS502 sub-program. *adf07* data can also be investigated separately by means of ADAS502.

The specific ion files contain detailed information on a large, but limited number of excited states up to $n = 3$ for most ions, $n = 4$ for neutral helium or, as in the case of hydrogen, up to $n = 5$. The influence of higher lying levels can be projected down by adding so-called expansion files, which contain the global information on a larger number of levels. Files in the central data base, which include projected information, are characterised by the letter *p*.

ADAS208 produces results in parameterized form as a function of T_e and n_e , which can be stored as *text* files containing the complete information on the program execution parameters and results for the various contributions to the excited state populations calculated by ADAS208. Groups of diagnostic lines can be chosen and their effective excitation contributions stored in the format of diagnostic line files (*pec*). The numbers of ionisation events per photon are available in the *sxb* data sets, if selected. It should be pointed out that the *pec.pass*

data sets from ADAS208 do not contain the number of transitions in the first line but have "???" instead. This line must be edited before usage in ADAS503. The *text* files are most useful and were interrogated in the context of the present analyses by means of a PC program. It is worthwhile mentioning that the ADAS208 graph only shows the ground state driven contribution. Finally, the general collisional radiative (*gcr*) files contain ionisation and recombination rate coefficients (*scd208.pass*, *acd208.pass* - no dielectronic recombination, format of *adf12*) computed from the *adf04* information. These coefficients are required for calculating the equilibrium ionisation balance and the corresponding excited level population due to recombination. They were used in this respect for the present analyses. It should be noted that the format of these files is substantially different from the usual processed data for code input in class *adf11*. Furthermore, if either the ionising or the recombining ion or both have metastable levels, several coefficients are produced linking every lower with every upper state. For hydrogen, this complication does not arise and is therefore not discussed here. The *gcr* files also give total line radiation and other ADAS208 information.

There are already many data sets generated by ADAS208 in the central ADAS data base, e.g. for diagnostic line radiation (*adf15*) or for ionisation events per photon (S/XB, *adf13*). They are characterised by the letter *u* or *r* for metastable-resolved or unresolved results (see below). The contributions to spectral lines stored in these data files refer to excitation from individual metastable levels *m*, to recombination or to charge exchange. Sometimes they are related to the total population of bound states and are then named *T* in the respective tables. In ADAS208 metastable-resolved results are being produced, if more than one metastable level is chosen (the proper ground state is considered as one metastable level). If the recombination option is chosen, threebody recombination contributions will always be computed. For including radiative recombination or charge exchange the relevant coefficients must be present in the input data set (not very often the case). If the value of ground and metastable state ionisation coefficients is very important, certainly for calculating S/XB ratios, but also e.g. for interpreting helium beam results, the "ionisation coefficient search" must be used. Since the selection of several metastable states is mandatory in these cases, ADAS208 will not generate unresolved data as a standard procedure. For fusion plasmas, ionisation out of excited levels should always be selected. In the case of neutrals and for high density divertor plasmas it is usually necessary to include recombination.

For taking into account the opacity of resonance lines, the transition probabilities in the relevant *adf04* input files were multiplied by the appropriate escape factors and the data were then processed by ADAS208 in the usual way.

Calculation of Escape Factors

For the plasma conditions under consideration, population of atomic excited states by photon absorption is an important process. As usual, absorption is treated as negative emission and the absorption rate is taken into account by subtracting it from the spontaneous emission rate,

$$\Theta = \frac{E - G}{E} = 1 - \frac{G}{E}. \quad (1)$$

The absorbed power G is proportional to the spectral radiance $L_\lambda(\lambda)$ at the plasma location considered and to the local effective absorption coefficient $\alpha'(\lambda)$. Here, α' represents the true absorption coefficient α minus the coefficient for stimulated emission, a convention, which is common when dealing with radiative transfer. In order to obtain the total emission and absorption power within a given spectral line, the spectral emission and absorption must be integrated over the wavelength λ and over the solid angle Ω . For that purpose, the spectral line profiles $P_\lambda(\lambda)$ are required, which must be calculated on the basis of the relevant line broadening mechanism in the plasma. For the emitted power the above double integration simply yields 4π times the line emission coefficient ϵ_L . The spectral radiance usually depends on the individual directions in the plasma as characterised by the solid angle element $d\Omega$:

$$\Theta = 1 - \frac{\int \int \alpha'(\lambda) L_\lambda(\lambda, \Omega) d\lambda d\Omega}{4\pi \epsilon_L} \quad (2)$$

The spectral radiance must be calculated by means of the equation of radiative transfer using the spectral emission coefficient $\epsilon_\lambda(\lambda)$ as a function of the plasma geometry. If the population is evaluated for position $\ell = 0$ and a is the distance to the plasma edge, where $L_\lambda = 0$, the radiance is given by

$$\frac{dL_\lambda}{d\ell} = \epsilon_\lambda - \alpha' L_\lambda \rightarrow L_\lambda(0) = \int_0^a \epsilon_\lambda(\ell) \exp\left[-\int_0^\ell \alpha'(\ell') d\ell'\right] d\ell. \quad (3)$$

The spectral absorption coefficient is given by the relation

$$\alpha(\lambda) = n_j \frac{g_k}{g_j} \frac{\lambda^4}{c} \frac{A_{kj}}{8\pi} P_\lambda(\lambda), \quad (4)$$

with the statistical weights g and the Einstein coefficient A_{kj} . Using a Doppler profile for the spectral line with a kinetic temperature T_0 and the relative ion mass μ of the emitters, the absorption coefficient in the line centre can be written as:

$$\alpha(0) = 1.08 \cdot 10^{-15} n_j \lambda f_{jk} \sqrt{\mu / T_0} \quad (f_{jk} = 1.5 \cdot 10^{-14} \lambda^2 \frac{g_k}{g_j} A_{kj}). \quad (5)$$

In Eq. (5) α is given in cm^{-1} with λ in nm, n_j in cm^{-3} and T_0 in eV. f_{jk} represents the absorption oscillator strength, which is introduced instead of the A -value here. The relation between A_{kj} and f_{jk} with λ in nm is added in brackets. The escape factor is finally obtained by integration over the spectral line profile and over all directions in the plasma, ultimately requiring a self-consistent solution of the whole problem.

For the calculations described below the following simplifying assumptions were made: Stimulated emission was neglected, i.e. $\alpha' = \alpha$, which is certainly well-justified for lines in the vuv and the relevant plasma conditions. A more serious restriction is the fact that the ground

state density was taken to be constant in the plasma resulting in a constant absorption coefficient α . For the spectral line profile Doppler broadening was adopted according to a neutral temperature T_0 , certainly only an approximation to the real broadening of neutral hydrogen lines, which is mainly due to Franck-Condon processes. The results were computed for the axis of a plasma cylinder of radius R , a geometry which had been used earlier for dealing with a plasma jet. A parabolic spatial profile was used for the radial dependence of the line emission coefficient. With these assumptions, the spectral radiance can be calculated analytically by an integration by parts, and the integration over spectral line profile and solid angle was performed numerically, with the option of using other profile shapes, as resulting from different line broadening mechanisms. For the purpose of calculating escape factors, a special PC code had been written earlier in BASIC (ADASESC.BAS) [3], [4].

The described program was employed to compute escape factors for hydrogen and for plasma conditions relevant to ASDEX Upgrade divertor plasmas. As a first example, the following parameters were used for the neutral temperature T_0 , the ground state density n_1 and the plasma geometry as characterised by the cylinder radius R : $n_1 = 5 \cdot 10^{13} \text{ cm}^{-3}$, $T_0 = 1 \text{ eV}$ and $R = 5 \text{ cm}$. A moderately optically thick case with $n_1 = 1 \cdot 10^{13} \text{ cm}^{-3}$ was investigated as well. The wavelengths and transition probabilities of the hydrogen lines were taken from the respective optically thin specific ion files, which will be referred to below in more detail. The results were displayed in the common way, i.e. relating the escape factor Θ to the product $\alpha(0) R$, where $\alpha(0)$ is the absorption coefficient in the line centre as given in Eq. (5) (proportional to n_1). Fig. 1 shows the escape factor in this normalised form, and the present results for the hydrogen Lyman lines for the above-mentioned plasma conditions are marked by the vertical dashed lines. As will be shown later, the population of the principal quantum number $n = 2$ is only of the order 10^{-6} of that of the ground state and therefore, the Balmer lines are not affected by self-absorption. As a further consequence, the ground state density n_1 is practically equal to the total neutral density n_0 . For calculating the optical thickness of transitions to excited states, their population can be taken into account in the escape factor program as a prescribed fraction of the Boltzmann distribution.

Hydrogen Ionisation Balance from of ADAS405 and adf11 Data.

Collisional-radiative ionisation and recombination rate coefficients for the optically thin case are provided within the ADAS system under the data group *adf11*. The convention for the filenames for ionisation and recombination coefficients is *scd<year>_<el>.dat* and *acd<year>_<el>.dat*, where *<el>* is the element symbol and *<year>* a two digit year number. The year "93" should be chosen, whenever available, otherwise there are default data sets (essentially the so-called Abel-van Maanen or Behringer data) bearing the year number "89". There are also metastable-resolved data designated by "93r", which are not being used in the codes at present. On the basis of these coefficients, the ionisation balance can be examined by means of ADAS405 as a function of the electron temperature T_e for a chosen electron density. ADAS405 does not provide the possibility to plot n_i/n_1 as a function of electron density; for that purpose a separate PC code was used based on the ADAS data retrieval subroutine *dhddata*, which allows reading coefficients for an array of temperatures and pertinent electron densities. In ADAS405, thermal charge exchange recombination can be included on the basis of *ccd<year>_<el>.dat* files. For charge exchange one must often resort to default

data sets, i.e. *ccd89_<el>.dat* etc.. Charge exchange was not considered in the present case. Fig. 2 shows an example of the hydrogen ionisation balance as a function of T_e for $n_e = 10^{14} \text{ cm}^{-3}$. For the discussion below it should be noted that the ionisation degree at 1 eV is about 5%.

In principle, the more sophisticated input data sets for ADAS405 like *<year> = "93" or "93r"* can also be reproduced on site, but this procedure has not been fully tested and until now this information has been drawn from the distributed files. In contrast, standard data are often being created within IPP Division E4 for new elements in the ASDEX Upgrade plasma experiments, as e.g. for nitrogen, fluorine, neon, chlorine or argon (note that some of the "89" data sets in the central ADAS data base are not correct, as is the case for argon). These data sets will eventually be part of the ADAS system, but at present they are stored under */u/kub/code_defaults* and bear the year number "00". It should be pointed out that the latter convention will be changed in the future to allow for *<year>* to be set to the year 2000.

ADAS405 also allows examination of the radiative power of each ionisation stage and the total radiation on the basis of *plt<year>_<el>.dat* (line radiation), *prb<year>_<el>.dat* (continuum radiation) and *prc<year>_<el>.dat* (charge exchange radiation) data sets. The discussion in the previous paragraph with respect to the choice of *<year>* and the availability of data sets also applies to these cases.

ADAS405 can e.g. be used to examine the influence of thermal charge exchange on the ionisation balance and the radiation of carbon impurities. It demonstrates that neutral densities of about $5 \cdot 10^9 \text{ cm}^{-3}$ are required to significantly change the hydrogen- and helium-like ion densities and to increase the total carbon radiation.

Optically Thin and Thick Hydrogen Ionisation Balance From ADAS208 Calculations

In the case of atomic hydrogen there are only L-resolved specific ion files available in the central data system. The mixing of levels within a specific principal quantum number n in the plasma takes place predominantly by ion collisions and can be included in principle in the ADAS system. However, it is justified to assume that the n -shells are fully mixed in the plasmas under consideration. For this case an n -bundled file can be produced by means of the program ADAS209. It should be noted that the recombination data are not bundled automatically but must be added-in by hand. The only central hydrogen file which contains radiative recombination data at present is *hlike_wjd92#h.dat*. It was used to produce */u/kub/adas/adf04/hlike/hbundle.dat* for the optically thin case and modified to apply to the optically thick plasma conditions described above by reducing the transition probabilities accordingly as */u/kub/adas/adf04/hlike/hbundle.thk* and */u/kub/adas/adf04/hlike/hbundle.thk1* for the moderately thick case. These files can be used like the others in ADAS208. No expansion file was used in the present analysis. The influence of radiative recombination was investigated by producing n -bundled files without these coefficients, i.e. */u/kub/adas/adf04/hlike/hbundleo.dat* and */u/kub/adas/adf04/hlike/hbundleo.thk* from *hlike_hps91h.dat*. For n -bundled hydrogen data it is of course pointless to ask for metastable-resolved calculations, but the metastable contribution is kept in the following formulas for completeness.

The hydrogen ionisation rate coefficients S calculated by ADAS208 on the basis of the above data sets with radiative recombination are shown in Fig. 3 as a function of electron density for $T_e = 1$ eV and $T_e = 2$ eV and for optically thick and thin conditions. Due to stepwise ionisation these rate coefficients increase in the density range 10^{12} to 10^{17} cm $^{-3}$ until the excited state population corresponds to the Boltzmann distribution, when S becomes again independent of n_e . The effectiveness of this process is shifted towards lower electron densities by the opacity of the resonance lines. Recombination rate coefficients α are plotted in Fig. 4 for the same variety of conditions. It may be somewhat surprising that they are also substantially modified by the plasma opacity. A detailed analysis, as shown in Fig. 5, demonstrates that radiative recombination directly into the ground state is the most important process at high temperatures ($T_e > 30$ eV) even for $n_e = 10^{14}$ cm $^{-3}$. However, at low temperatures and electron densities above about 10^{14} cm $^{-3}$, threebody recombination into the hydrogen excited states and subsequent emission of Lyman line photons represents the main contribution to the total recombination rate. Reducing the relevant transition probabilities by means of escape factors makes these channels less effective and therefore reduces the integral recombination coefficient. At very high densities, there is always the transition to the collision-dominated Boltzmann distribution, threebody recombination into all levels becomes more and more important and α eventually increases proportional to n_e due to its definition as a radiative coefficient. The discussed ionisation and recombination data could easily be used in plasma simulation codes to cope with optically thick plasmas. However, calculation of the actual opacity eventually requires a self-consistent radiation transport model in these codes.

The resulting ionisation balance n_i / n_1 is shown in Fig. 6 as a function of electron temperature and for $n_e = 10^{14}$ cm $^{-3}$. It is a steep function of T_e and remains well below Saha equilibrium even for the present optically thick case (Saha equilibrium requires $n_e \approx 10^{16}$ cm $^{-3}$). The ionisation degree as a function of electron density will be discussed below.

The present results for S and α are somewhat different from the ADAS "93" data, particularly at low electron temperatures and densities. Both "93" data are up to a factor of two high. This discrepancy is most likely due to a different *adf07* coefficient for the hydrogen ground state ionisation and is being investigated.

Excited State Population from the Collisional-Radiative Code ADAS208

ADAS208 computes the collisional-radiative population coefficients C_x^y for excited states of a specific atom or ion. There are four contributions to the population, namely, electron impact excitation from the ground and metastable levels of the same ion z , designated by the index z, m ($m = 1$ for the ground state), recombination of free electrons and ions in their ground or metastable states of the next ionisation stage $z+1, v$, charge exchange of these ions in their ground or metastable state with neutral hydrogen or helium, and ionisation of ions in ground or metastable states of the previous ionisation stage $z-1, w$:

$$n_{z,k} = \sum_m n_{z,m} C_{k,m}^{excit} + \sum_v n_e n_{z+1,v} C_{k,v}^{recom} + \sum_v n_{z+1,v} n_H C_{k,v}^{CX} + \sum_w n_e n_{z-1,w} C_{k,w}^{ion} \quad (6)$$

The excitation part can refer to several metastable levels with densities n_m which can be followed individually in plasma transport codes (metastable-resolved results) or can be related to an equilibrium metastable population (unresolved data). In order to reduce resolved data to unresolved data the equilibrium metastable population must be calculated

$$n_{z,m>1} = n_{z,1} C_{m,1}^{excit} + \sum_v n_e n_{z+1,v} C_{m,v}^{recom} + \sum_v n_{z+1,v} n_H C_{m,v}^{CX} + \sum_w n_e n_{z-1,w} C_{m,w}^{ion} \quad (7)$$

and inserted in Eq. (6). For n-bundled hydrogen data there are no metastable states and the level number k is equal to the principal quantum number n of the excited state. There are not metastable ion states, either, and n_{z-1} does not exist. In those equations, which only refer to hydrogen, n_n is being used for $n_{z=0,n}$ and n_i for the only state of $n_{z+1=1}$.

Excitation, recombination and possibly charge exchange contributions to the intensities of diagnostic lines can be examined by means of ADAS503. The central ADAS data base contains information on many diagnostic lines of various elements and ionisation stages. Their information has been interrogated frequently for carbon lines observed in ASDEX Upgrade and compared to earlier data in the transport codes. Since these were based on a previous version of ADAS, it is not surprising that, as a rule, they perfectly agree with the new values.

The contributions to the H_α radiation, computed in this study, can be investigated after producing a *pec.pass* file by ADAS208. Examples for the excitation and recombination contributions for the optically thin and the optically thick cases are shown in Fig. 7 and 8 as a function of electron temperature at $n_e = 10^{14} \text{ cm}^{-3}$. In order to obtain photon numbers per s and cm^{-3} , the quantity in Fig. 7 must be multiplied by n_i and n_e , that in Fig. 8 by n_i and n_e . The two pairs of curves demonstrate the influence of radiative recombination, Fig. 8 shows directly the relative magnitudes of radiative and threebody recombination (files *hbundle.dat*, *hbundleo.dat*, *hbundle.thk* and *hbundleo.thk*). The relative importance of the recombination contribution can be derived from Fig. 8 by multiplying the coefficients by the ionisation degree n_i/n_1 and comparing them to the values in Fig. 7. The ADAS208 *text* output lists the coefficients for the level population as given in Eq. (6). Therefore, in order to reproduce the data in Figs. 7 and 8, the excitation coefficient must be divided by n_e and both contributions must be multiplied by the relevant transition probability.

It is found that, at least for higher principal quantum numbers and at low temperatures, the hydrogen excited level densities depend mainly on n_e and n_i and to a lesser extent on the ground state excitation, which means that the ionisation balance must be known for computing the excited state numbers. For an investigation of equilibrium plasma conditions, i.e. without particle transport, the ADAS208 ionisation balance was used to calculate hydrogen excited level populations. The corresponding results for principal quantum numbers 2 to 5 are shown in Figs. 9 and 10 as a function of electron density. They are presented in the usual form $n_n/n_1 n_e$, a quantity, which is independent of n_e in corona balance and falls with $1/n_e$ in Boltzmann equilibrium. With increasing n_e , corona balance changes to Boltzmann equilibrium at $n_e \approx 10^{17} \text{ cm}^{-3}$. In the optically thick case, of course, Boltzmann equilibrium is reached

at lower electron densities.

A comparison of Fig. 9 and Fig. 10 demonstrates that, for the same plasma parameters, the radiation of H_α and other lines can be increased by about a factor ten due to the plasma opacity, although the lines themselves are completely or approximately optically thin (only L_α is really optically thick). Therefore, the effect might go undetected experimentally by a comparison of H_α to L_β line radiation. The population takes place via a higher ionisation degree, as demonstrated in Fig. 6 for a still moderate electron density. This mechanism could possibly explain the high H_α radiation observed in ASDEX Upgrade discharges close to the density limit.

The relative contribution of recombination with respect to ground state excitation is an important issue in the analysis of Balmer line radiation and depends on the above coefficients but also on the actual densities of ions, electrons and neutral atoms. It will be dealt with below in more detail. If recombination into and ionisation out of excited states are the dominant processes, the excited state population n_n corresponds to its Saha equilibrium value calculated from n_e , n_i and T_e on the basis of the Saha equation. If all levels considered are in Saha equilibrium (collision limit lower than the relevant n , i.e. partial local thermodynamic equilibrium, PLTE), they allow measurement of the electron temperature from the slope of a so-called Boltzmann plot, i.e. plotting the logarithm of excited state numbers divided by their statistical weights against excitation energy. Such a presentation is shown in Fig. 11 together with the PLTE line for the ionisation balance given by atomic physics. It should be noted that for 1 eV and 10^{14} electrons per cm^{-3} , the neutral density has the unrealistically high value of $2.3 \cdot 10^{15} \text{ cm}^{-3}$. All levels shown are quite close to their equilibrium values, the ones with $n = 3-5$ are even over-populated due to the unbalanced radiative recombination processes. With increasing n they approach again the PLTE line. PLTE is of course better realised at higher electron densities.

Approximate Calculation of Line Intensities and Ionisation Balance

For an approximate analysis, a method can be used which is based on the following considerations. Eq. 6 can be rewritten in the following form

$$\frac{n_{z,k}}{n_{z,1}} = C_{k,1}^{\text{excit}} + \sum_{m>1} \frac{n_{z,m}}{n_{z,1}} C_{k,m}^{\text{excit}} + \sum_v \frac{n_e n_{z+1,v}}{n_{z,1}} C_{k,v}^{\text{recom}} + \dots, \quad (8)$$

where $\frac{n_e n_{z+1,v}}{n_{z,1}} = f(T_e)$, but independent of n_e for Saha equilibrium, and

$$\frac{n_{z,m}}{n_{z,1}} = C_{m,1}^{\text{excit}} + \sum_v \frac{n_e n_{z+1,v}}{n_{z,1}} C_{m,v}^{\text{recom}} + \dots. \quad (9)$$

Since the assumption of Saha ionisation balance with respect to the ground state is certainly not justified in the considered plasmas, Eq. (8) is further modified to yield:

and, neglecting charge exchange and direct ionisation into the excited state, the following formula is found for the population of excited states $n_{z,k}$ with respect to the ground state $n_{z,1}$:

$$\frac{n_{z,k}}{n_{z,1}} = \frac{C_{k,1}^{excit} + \sum_{m>1} \frac{n_{z,m}}{n_{z,1}} C_{k,m}^{excit}}{1 - \sum_v \frac{n_e n_{z+1,v}}{n_{z,k}} C_{k,v}^{recom}} \quad (11)$$

The ratio $n_e n_{z+1,1} / n_{z,k}$ is very close to the respective equilibrium relation for higher principal quantum numbers n (for hydrogen $k = n$) and higher electron densities. The other metastable ion states may either be neglected or considered to be statistically populated. Therefore, $n_{z,k}$ can now be computed without knowing n_e and n_{z+1} on the basis of the PLTE relation (Saha equation for the excited states). This method is identical to omitting both ionisation and recombination in the ADAS calculations in the first place, a method used in earlier analyses based on the code ADAS205 [3, 4].

In principle, Eq. (11) can also be used to calculate the population of metastable levels in a system like helium. However, the assumption of PLTE is usually not very well fulfilled for these states. They are dominated by the ground state excitation and are over-populated with respect to PLTE. The same may be true for excited levels, which have a normal transition probability to the ground state, but where the resonance lines are very optically thick. It is better to adopt Boltzmann population or a prescribed fraction thereof for the population of the metastable levels.

As a further step in the approximate analysis, the product $n_e n_{z+1}$ can be calculated from the known ratio $n_{z,k} / n_{z,1}$ using the PLTE relation. This means that the electron and ion densities are essentially determined by excitation and subsequent ionisation.

The optically thin ionisation balance for hydrogen from the above method is shown in Fig. 12 as a function of electron density for $T_e = 1$ eV in comparison to n_i / n_1 on the basis of the ADAS208 collisional-radiative ionisation and recombination data. The agreement of the present analysis with the latter results is excellent for higher electron densities and for higher hydrogen n -values and confirms the validity of the PLTE assumption in this range. The ionisation degree is around 5% for electron densities applicable to fusion plasmas and drops slowly for lower and higher densities. The present optically thick conditions (neutral density $n_0 = 5 \cdot 10^{13} \text{ cm}^{-3}$) have been examined using the same method and the result for the hydrogen ionisation balance is shown in Fig. 13, again as a function of n_e and for $T_e = 1$ eV.

Neutral Hydrogen Density Measurements Using the Intensities of the Balmer Lines

Sometimes electron densities and temperatures in divertor plasmas are known, e.g. from hydrogen Balmer continuum measurements, and the question is, whether the Balmer lines contain additional information on the number of neutral hydrogen atoms. To deal with this problem, the present results have been re-compiled for a given electron density and temperature, but for various neutral densities n_0 . Fig. 14 shows the corresponding result for optically thin

conditions and electron temperatures of 1 eV and 1.5 eV. The excited state numbers with $n = 3-5$ are presented relative to their equilibrium population, as discussed above. This ratio is always very close to one for neutral densities corresponding to the equilibrium ionisation balance. At low neutral population the excitation contribution becomes negligible, and at $n_e = 10^{14} \text{ cm}^{-3}$ the excited states have about 50% of their equilibrium value independent of n_0 . Of course, no information on n_0 can be obtained in this case. If n_0 is over-populated, this shows very clearly in the excited states, particularly in $n = 3$ (H_α). However, the electron temperature has a very strong influence on the transition and must be known precisely. For optically thick conditions the results are shifted in density, but otherwise similar, as shown in Fig. 15.

For the ASDEX Upgrade divertor and high electron densities n_0 is expected from code calculations to be around 10^{13} cm^{-3} . This means that the hydrogen Lyman lines are moderately thick at most and Fig. 14 applies rather than Fig. 15. If the electron temperatures are as low as 1 eV, the described measurement of neutral hydrogen atoms is impossible and about half the equilibrium population should be found from the first Balmer lines. The Boltzmann plot is expected to look like the graph shown in Fig. 16, a confirmation of which appears highly desirable. On the other hand, if the neutral density were an order of magnitude higher, the Lyman lines would be considerably optically thick with a pertinent change in ionisation degree. The divertor plasma could then just be in ionisation equilibrium as predicted by atomic physics and no net recombination would take place.

For the first condition, discussed above, the neutral density is two orders of magnitude below the atomic physics equilibrium value of $2.33 \cdot 10^{15} \text{ cm}^{-3}$, which means that the plasma is strongly recombining. The effective recombination rate can be easily calculated from Figs. 4 and 5 to be about $2 \cdot 10^{15} \text{ cm}^{-3} \text{ s}^{-1}$ at $n_e = n_i = 10^{14} \text{ cm}^{-3}$. The spatial extension of this region along field lines is of the order of 2 m (5 - 10 cm poloidally), as shown by B2-Eirene calculations [5] as well as measurements [6], and the particle sink strength due to recombination will therefore be some $10^{17} \text{ cm}^{-2} \text{ s}^{-1}$. This number must be compared with the particle flux down into the divertor. Thus, if the flow velocity is comparable to the sound speed and the flux density some $10^{19} \text{ cm}^{-2} \text{ s}^{-1}$, recombination represents only a very small perturbation to the total particle losses. It will only play a significant role, if the flow slows down to very low velocities, or if the recombination rate is substantially enhanced by other processes, e.g. molecular recombination channels. These statements are in complete agreement with code calculations [5].

Summary

The ADAS208 atomic physics code (collisional-radiative model) was employed to calculate excitation, ionisation and recombination coefficients for neutral hydrogen for optically thin and optically thick plasma parameters. Most of the required input data were available in the relevant specific ion files in group *adf04* of the ADAS data base. The detailed level information had to be n -bundled first using the ADAS program ADAS209. The optical thickness of resonance lines was taken into account by reducing the optically thin transition probabilities, i.e. by multiplying them by an escape factor $\Theta \leq 1$. Escape factors for ASDEX Upgrade density limit plasma conditions were calculated by means of a PC program on the basis of some simplifying assumptions.

Ionisation and recombination rate coefficients for optically thin plasmas and two cases of opacity were generated by ADAS208. They demonstrate the effects of stepwise ionisation and recombination into excited levels, which are a function of the optical thickness of the Lyman lines. There is some unresolved discrepancy between the present optically thin coefficients and the ones stored in the ADAS data base. The ADAS208 coefficients were used to calculate the equilibrium ionisation balance and recombination contribution to excited level population. They are also available for plasma simulation codes. In the electron density range between 10^{12} and 10^{17} cm^{-3} the excited states show the transition from Corona to Boltzmann equilibrium, which occurs earlier in cases of optically thickness, as is to be expected. A comparison of the results for the optically thin and thick cases demonstrates that the opacity of (essentially) L_α leads to an increase in ionisation degree of almost an order of magnitude and to a similar enhancement in hydrogen line radiation for the relevant plasma conditions. Still, the described opacity effects may go undetected in an experimental study of H_α versus L_β radiation. It is therefore very worth-while to include optical thickness in divertor plasma simulations.

Above $n_e \approx 10^{14} \text{ cm}^{-3}$ the hydrogen excited states with principal quantum numbers n greater than 2 are close to Saha equilibrium with electrons and ions (PLTE), if the neutral density is not far from the atomic physics equilibrium value. This allows a T_e analysis by means of a Boltzmann plot and an approximate calculation of the ionisation balance without explicitly using the ionisation and recombination coefficients. In essence, this procedure was used in earlier analyses of nitrogen lines based on the code ADAS205.

The excitation and recombination coefficients calculated by ADAS208 were analysed to separate the two contributions to spectral line emission for ionisation degrees far from equilibrium. If the ground state excitation is significant, the plasma neutral density can be measured from the Balmer spectral line emission. However, it was found that the electron temperature must be known precisely for this procedure, and that most likely the neutral density cannot be determined in this way in the ASDEX Upgrade divertor and for density limit conditions, because it is too low. These plasmas are probably characterised by volume recombination, but recombination only plays a role as a particle sink if the flow velocities are substantially below sound speed.

In the course of the data analysis and display, other ADAS codes were used to interrogate atomic physics data sets, namely, ADAS405 for the collisional-radiative ionisation balance and radiation contributions, ADAS503 to plot contributions to individual line radiation, ADAS502 to investigate zero-density ionisation rate coefficients and ADAS501 to interrogate ionisation events per photon SXB. The main analysis was done by on the basis of the ADAS208 *text* output by means of a PC program.

References:

- [1] F.E. Irons, The Escape Factor in Plasma Spectroscopy - I. The Escape Factor Defined and Evaluated, JQSRT 22, 1 (1979)
- [2] H.P. Summers, L. Wood, Ionisation, Recombination and Radiation of Impurities in Plasmas, JET Report, JET-R(88)06 (1988), ADAS Data Pool (Atomic Data and Analysis Structure), Editor H.P. Summers (1993)
- [3] SFB 259, Bericht über Hochtemperaturprobleme rückkehrfähiger Raumtransport-systeme, Arbeits-u. Ergebnisbericht, Universität Stuttgart, 1992
- [4] H. Jentschke, Spektroskopische Untersuchung eines luftähnlichen Plasmafreistrahls, Thesis, Institut für Plasmaforschung, Universität Stuttgart, 1995
- [5] R. Schneider, private communication 1997
- [6] B. Napiontek, private communication 1996

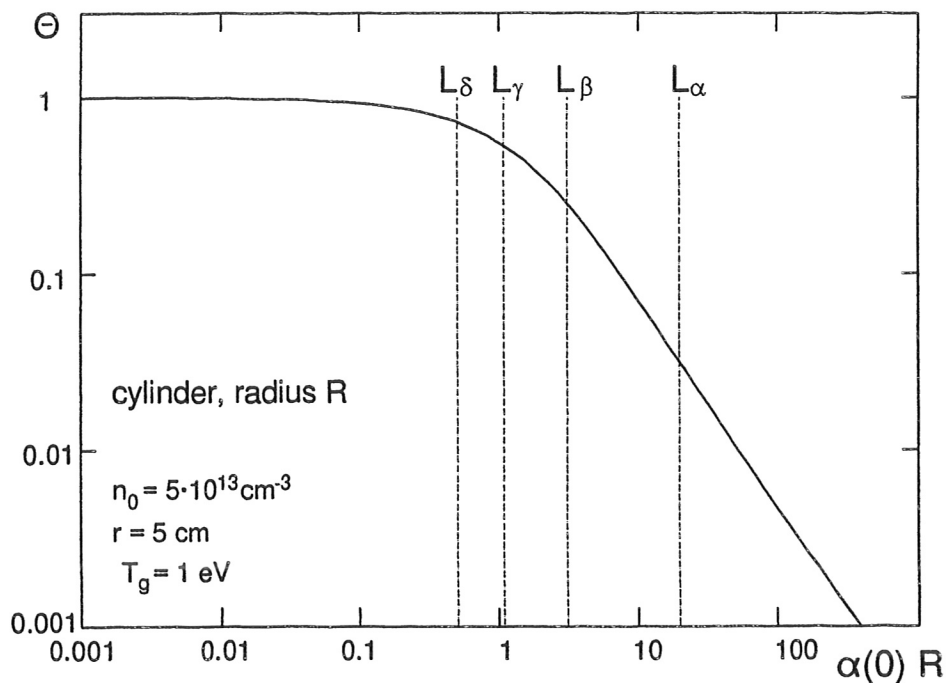


Fig. 1: The escape factor Θ on the axis of a plasma cylinder of radius R as a function of the optical depth in the line centre $\alpha(0) R$. Doppler broadening is assumed for the line. The optical depths of some Lyman lines are marked for the present optically thick conditions, i.e. $n_0 = 5 \cdot 10^{13} \text{ cm}^{-3}$, $T_0 = 1 \text{ eV}$, $R = 5 \text{ cm}$.

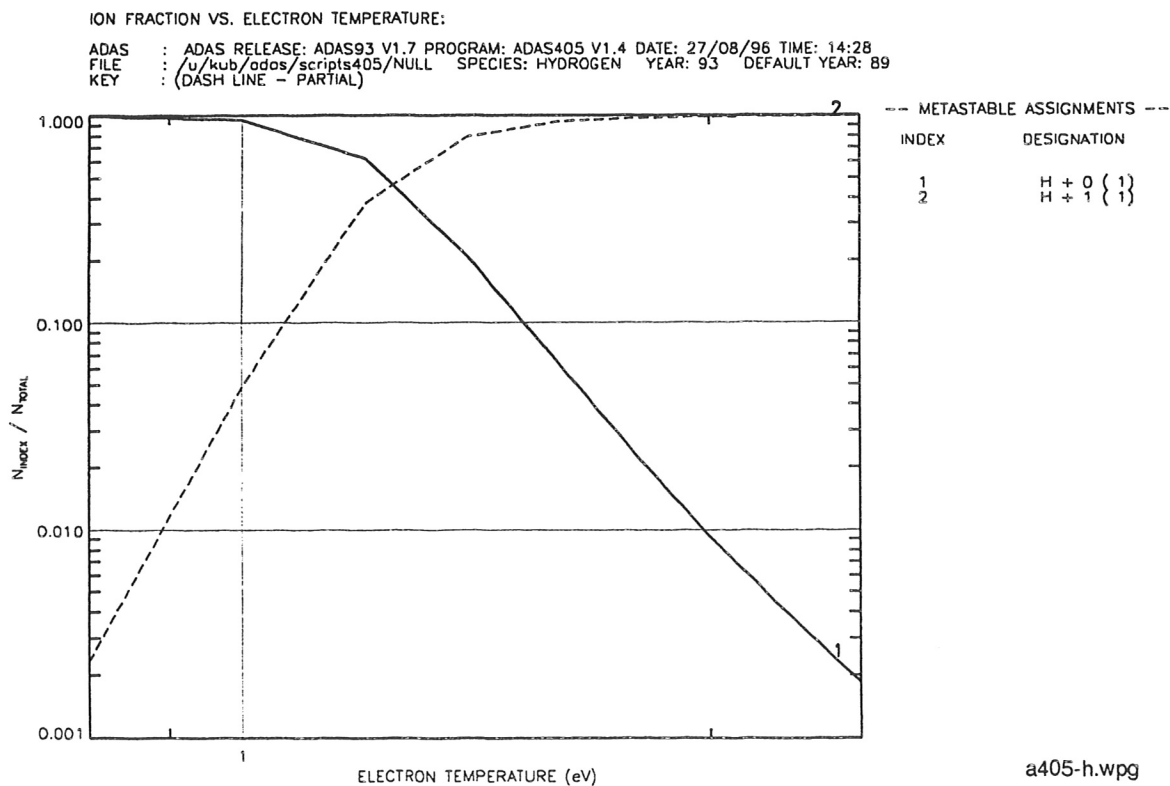


Fig. 2: Ionisation balance for hydrogen as a function of T_e on the basis of the ADAS data sets *scd93_h.dat* and *acd93_h.dat*, $n_e = 10^{14} \text{ cm}^{-3}$. The graph was produced by ADAS405.

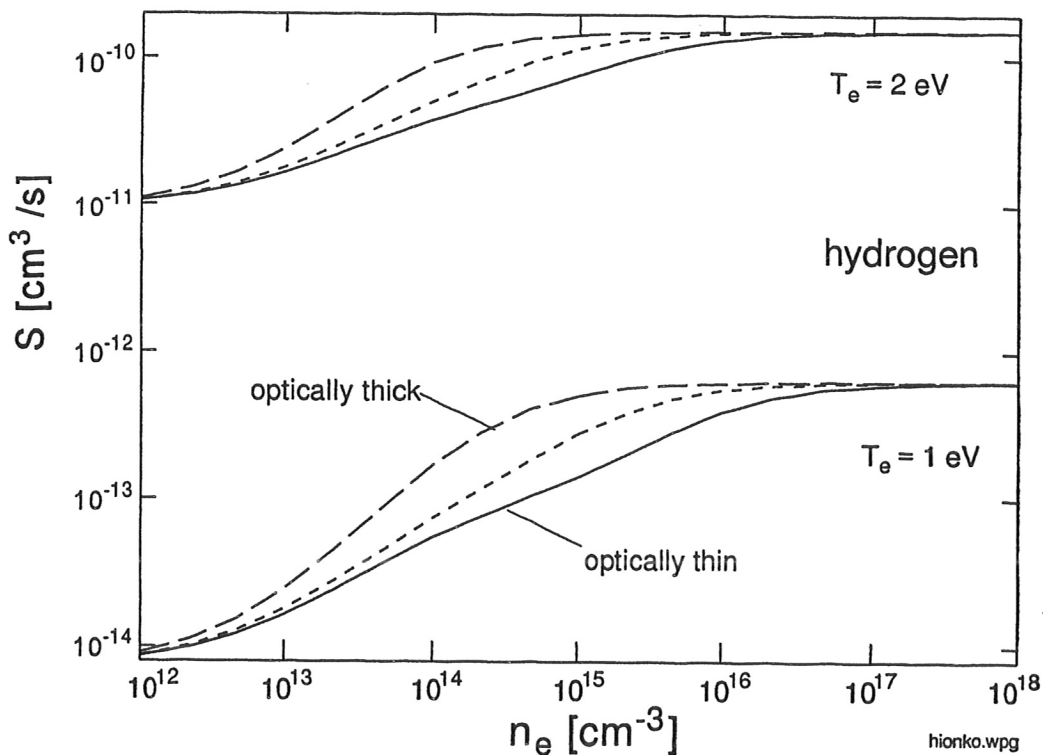


Fig. 3: Ionisation rate coefficients S for hydrogen as a function of electron density calculated by ADAS208 (*scd208.pass*). Optically thin as well as optically thick cases with $n_0 = 1 \cdot 10^{13} \text{ cm}^{-3}$ and $n_0 = 5 \cdot 10^{13} \text{ cm}^{-3}$.

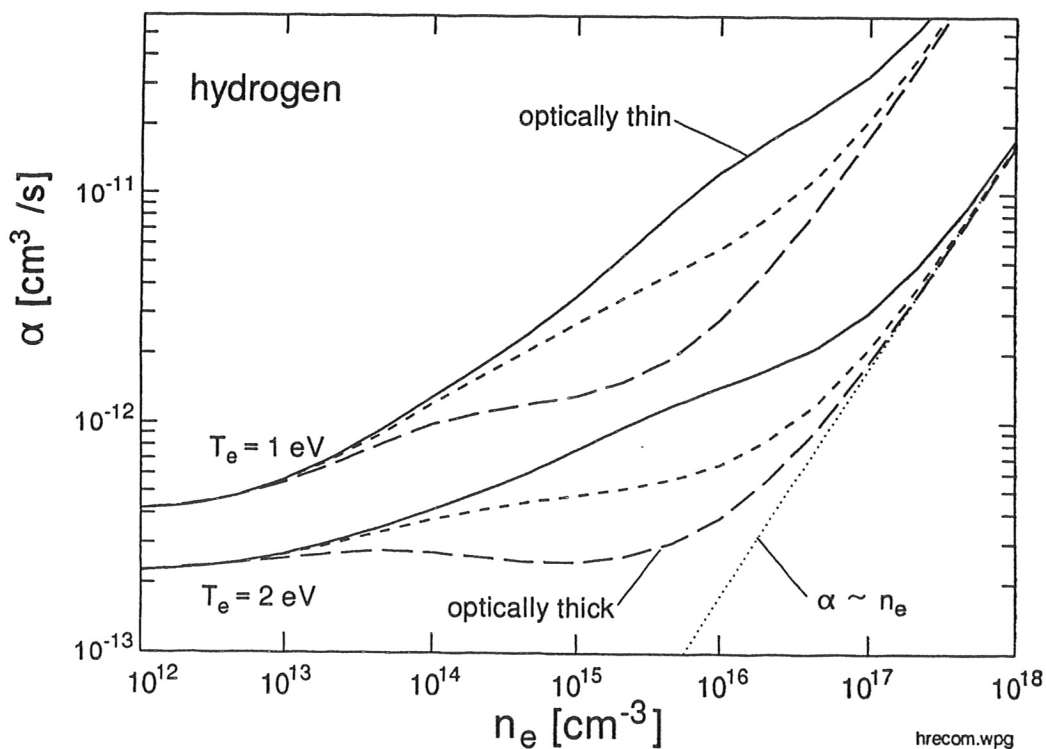


Fig. 4: Recombination rate coefficients α for hydrogen as a function of electron density calculated by ADAS208 (*acd208.pass*). Optically thin case as well as optically thick

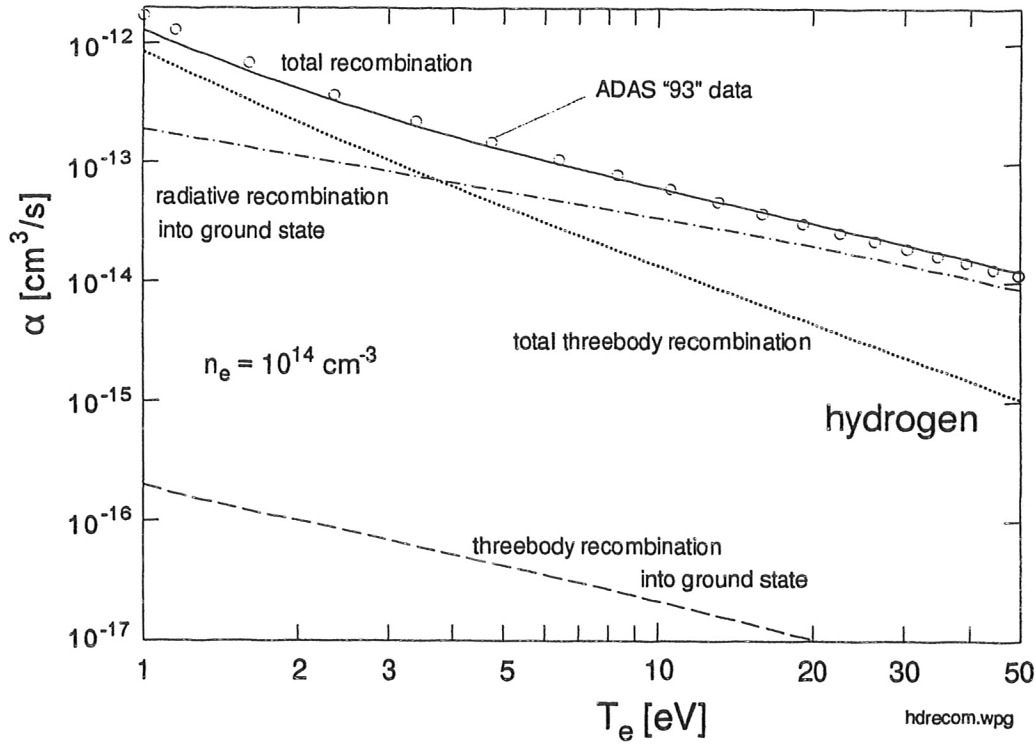


Fig. 5: Contributions to the total hydrogen recombination coefficient as a function of electron temperature, $n_e = 10^{14}$ cm⁻³. Data from the ADAS data base are also shown.

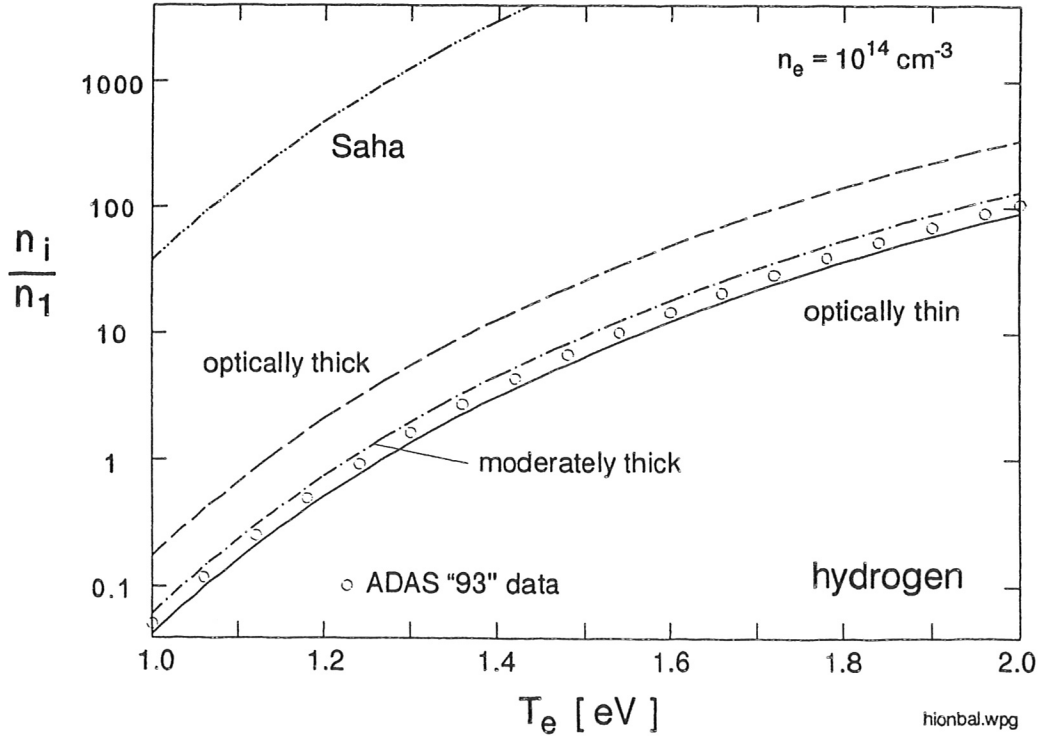
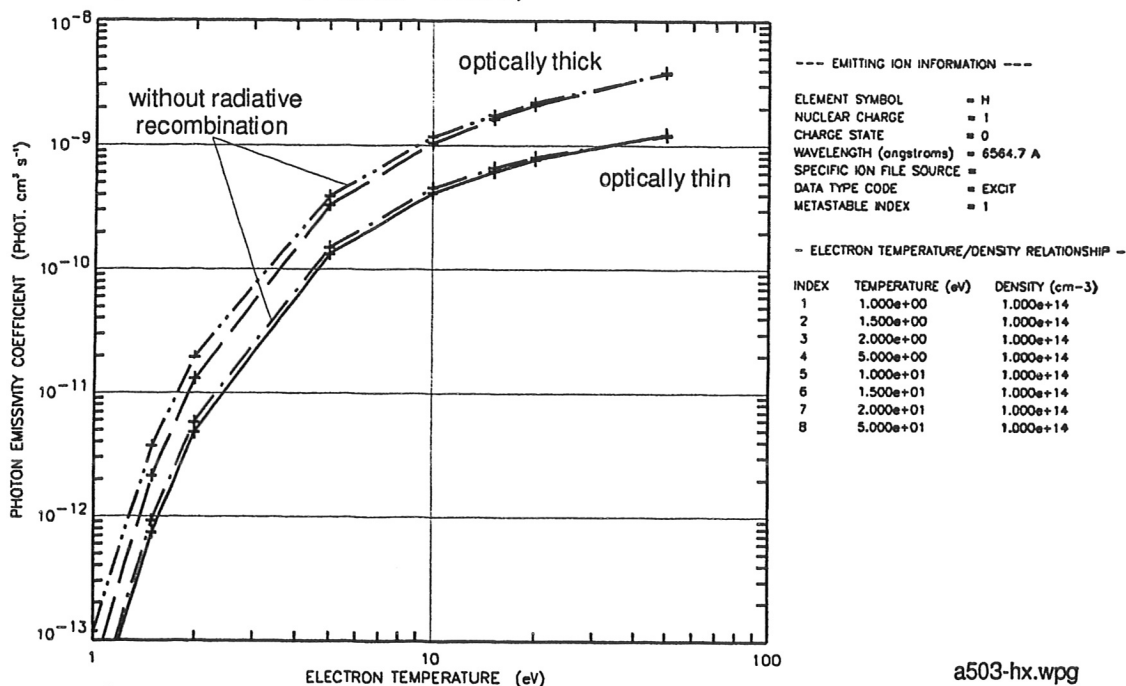


Fig. 6: Hydrogen ionisation balance as a function of T_e from the ionisation and recombination coefficients in Figs. 3 and 4, and from optically thin ADAS standard data, $n_e = 10^{14}$ cm⁻³. Saha equilibrium is also shown.

PHOTON EMISSIVITY COEFFICIENT VS ELECTRON TEMPERATURE

ADAS : ADAS RELEASE: ADAS93 V1.7 PROGRAM: ADAS503 V1.7 DATE: 09/09/96 TIME: 14:55
 FILE : /u/kub/adas/pos/hbundleo.thk.pass BLK= 5;H + 0 WAVELENGTH= 6564.7 A MET=1
 KEY : (CROSSES - INPUT DATA) (FULL LINE - SPLINE FIT)

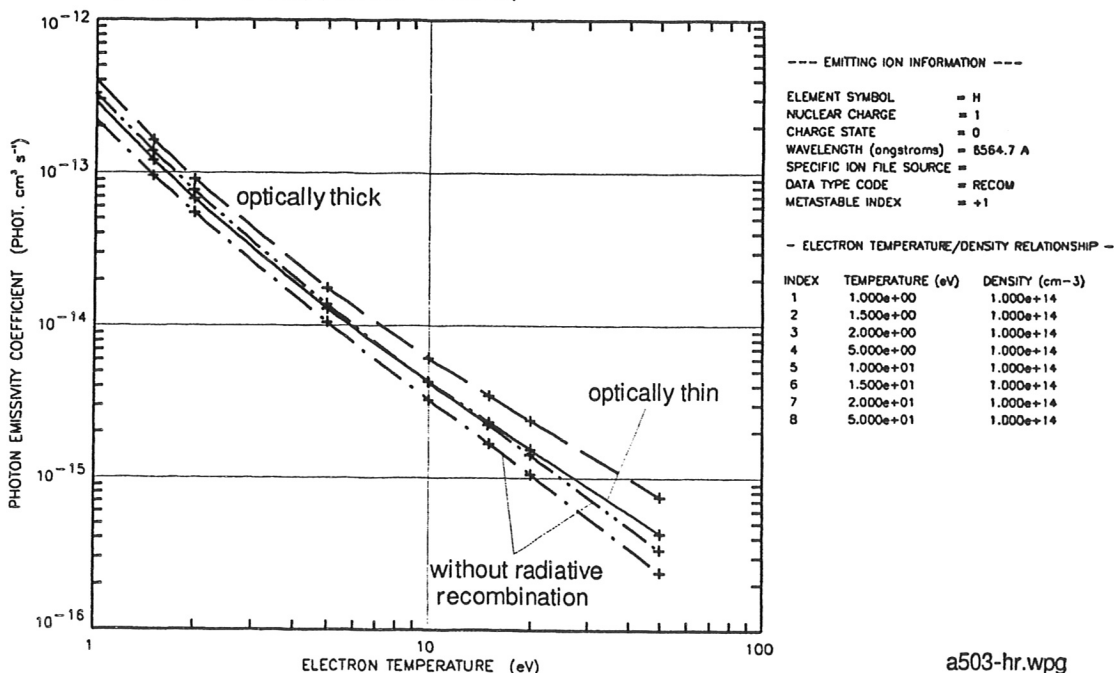


a503-hx.wpg

Fig. 7: Photon emissivity coefficients for Balmer- α as a function of T_e displayed by ADAS503. Excitation contributions, optically thin case and optically thick case ($n_0 = 5 \cdot 10^{13} \text{ cm}^{-3}$). The "pec" data were stored by ADAS208 using *hbundle.dat*, *hbundleo.dat*, *hbundle.thk* and *hbundleo.thk*, $n_e = 10^{14} \text{ cm}^{-3}$.

PHOTON EMISSIVITY COEFFICIENT VS ELECTRON TEMPERATURE

ADAS : ADAS RELEASE: ADAS93 V1.7 PROGRAM: ADAS503 V1.7 DATE: 09/09/96 TIME: 14:55
 FILE : /u/kub/adas/pos/hbundleo.thk.pass BLK= 15;H + 0 WAVELENGTH= 6564.7 A MET=+1
 KEY : (CROSSES - INPUT DATA) (FULL LINE - SPLINE FIT)



a503-hr.wpg

Fig. 8: Photon emissivity coefficients for Balmer- α as a function of T_e displayed by ADAS503.

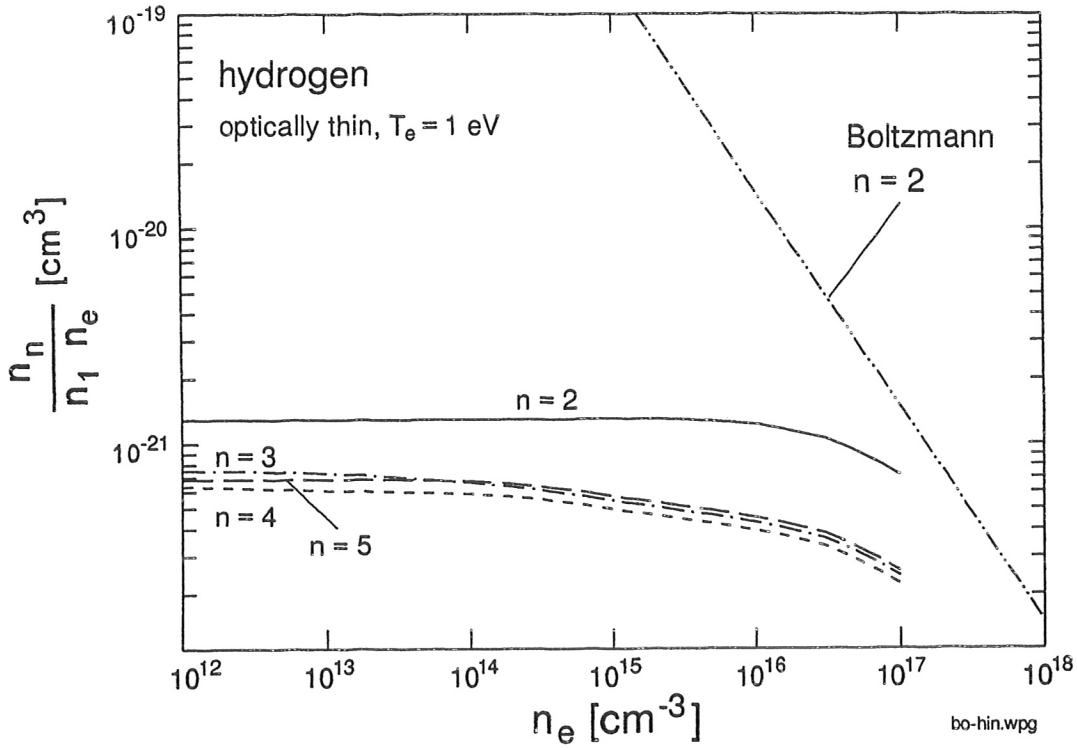


Fig. 9: Normalised population of excited hydrogen levels with principal quantum numbers n as a function of n_e . Optically thin case. Boltzmann equilibrium is plotted for $n = 2$.

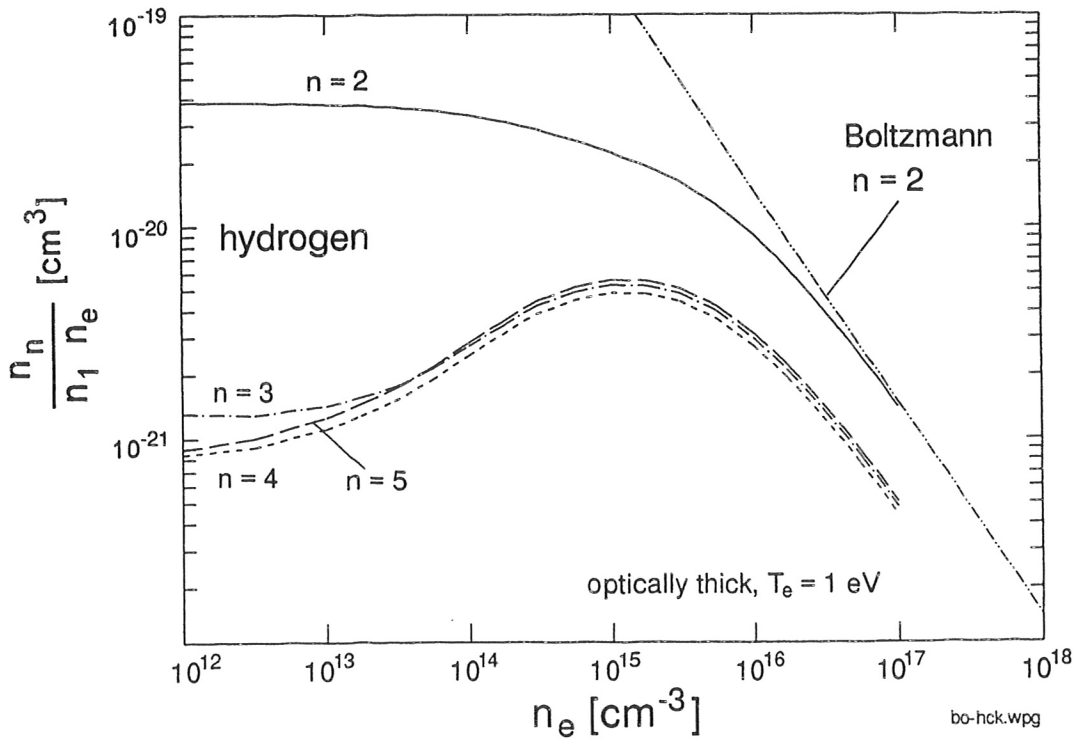


Fig. 10: Normalised population of excited hydrogen levels with principal quantum numbers n as a function of n_e . Optically thick case, $n_0 = 5 \cdot 10^{13} \text{ cm}^{-3}$. Boltzmann equilibrium is plotted for $n = 2$.

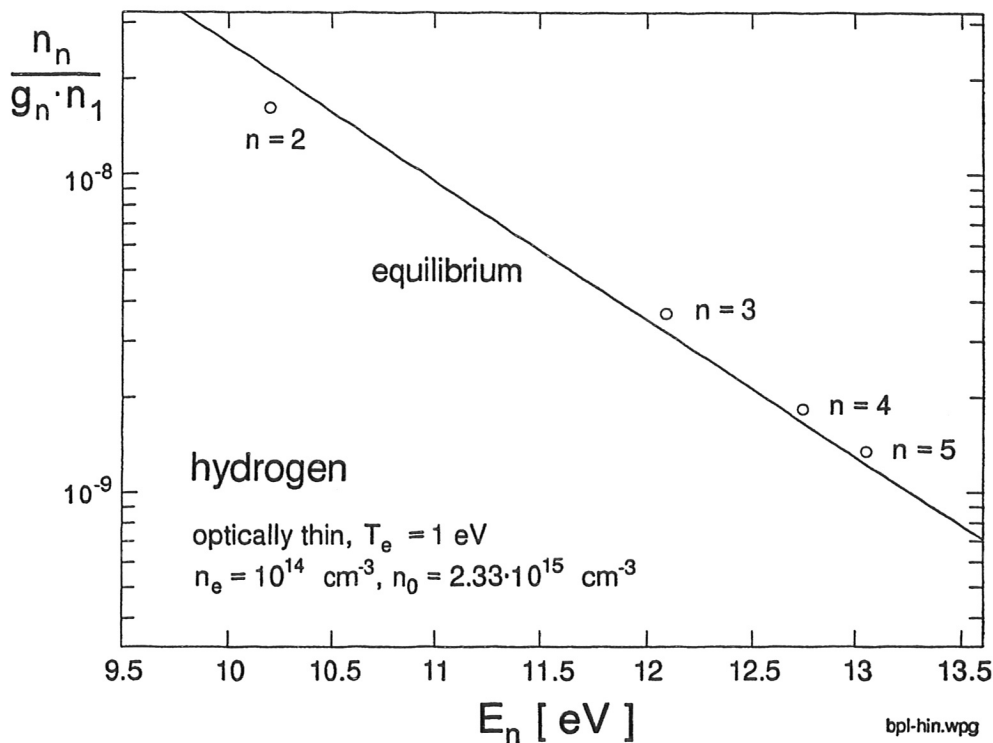


Fig. 11: Boltzmann plot of excited hydrogen levels for the indicated conditions. Saha equilibrium with electrons and ions is also shown.

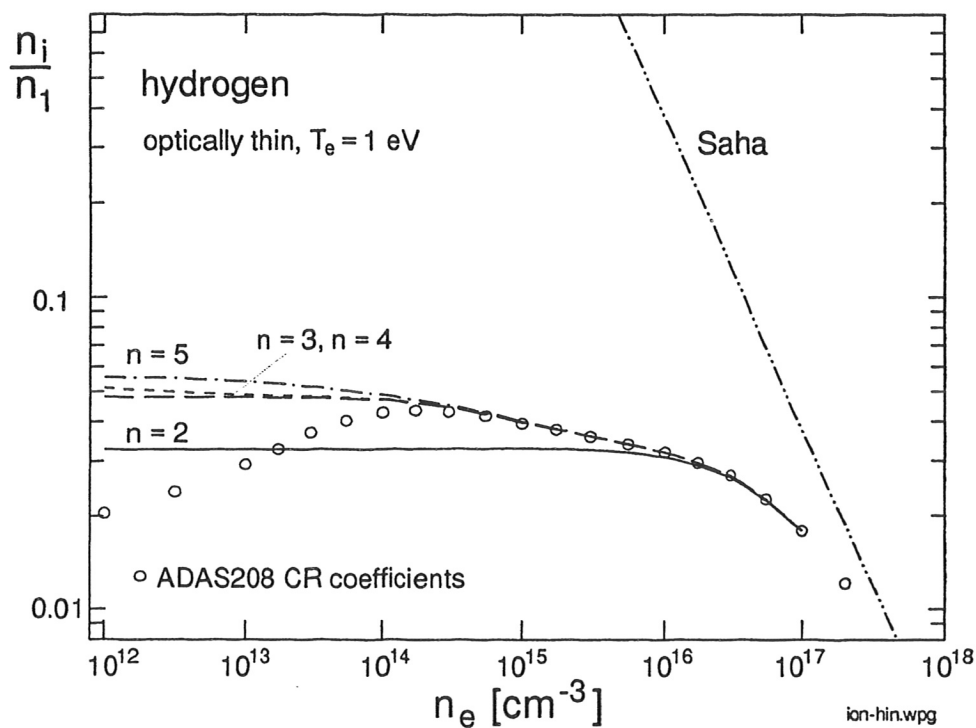


Fig. 12: Ionisation degree n_i/n_1 as a function of electron density. Shown are the results of the ADAS collisional-radiative (CR) ionisation and recombination coefficients as well as values from the approximate analysis assuming equilibrium excited level population.

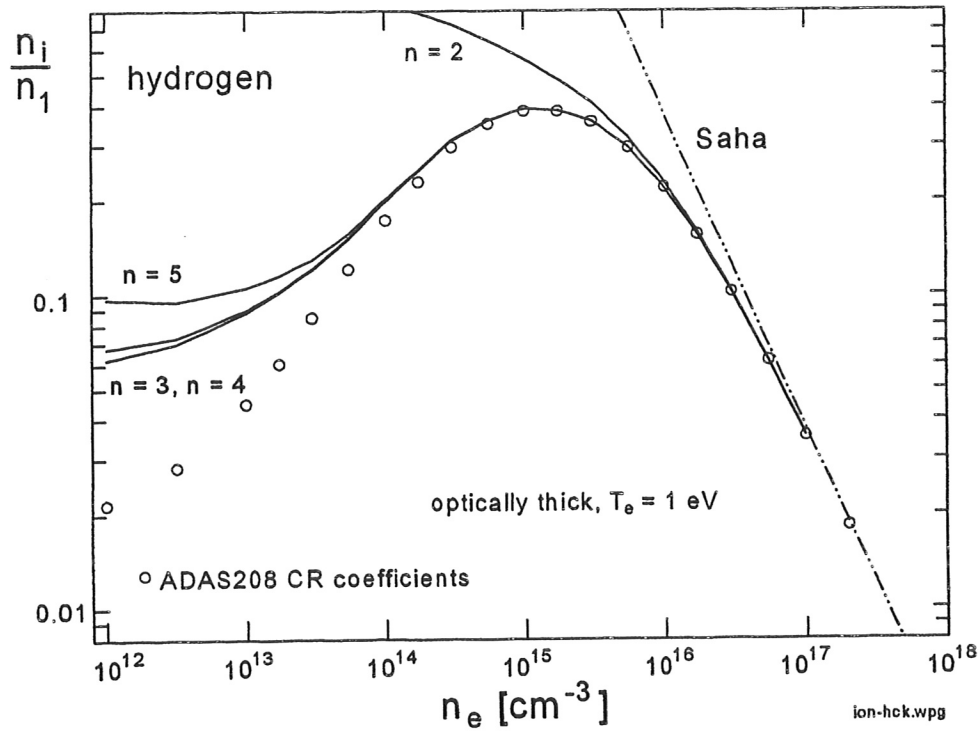


Fig. 13: Ionisation degree n_i/n_1 as a function of n_e for $T_e = 1 \text{ eV}$ from the approximate analysis and ADAS data as Fig. 12. Optically thick case, $n_0 = 5 \cdot 10^{13} \text{ cm}^{-3}$.

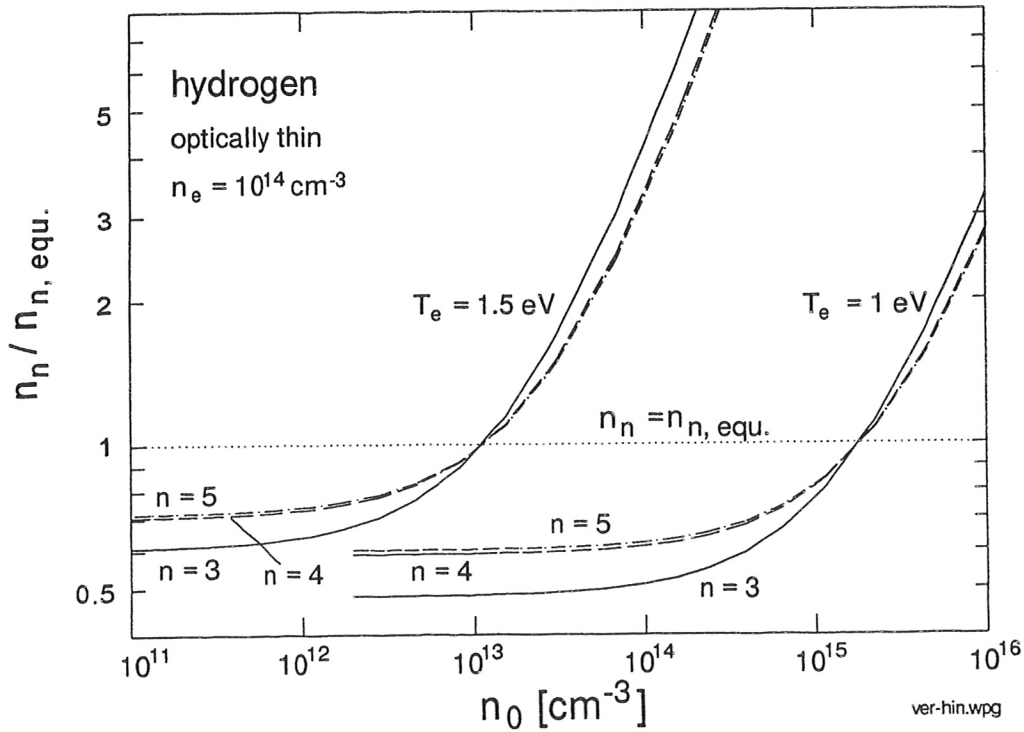


Fig. 14: Population of excited hydrogen levels with respect to their equilibrium population as a function of n_0 . Optically thin case. The equilibrium neutral densities are $1.65 \cdot 10^{13} \text{ cm}^{-3}$ for 1.5 eV and $2.33 \cdot 10^{15} \text{ cm}^{-3}$ for 1 eV.

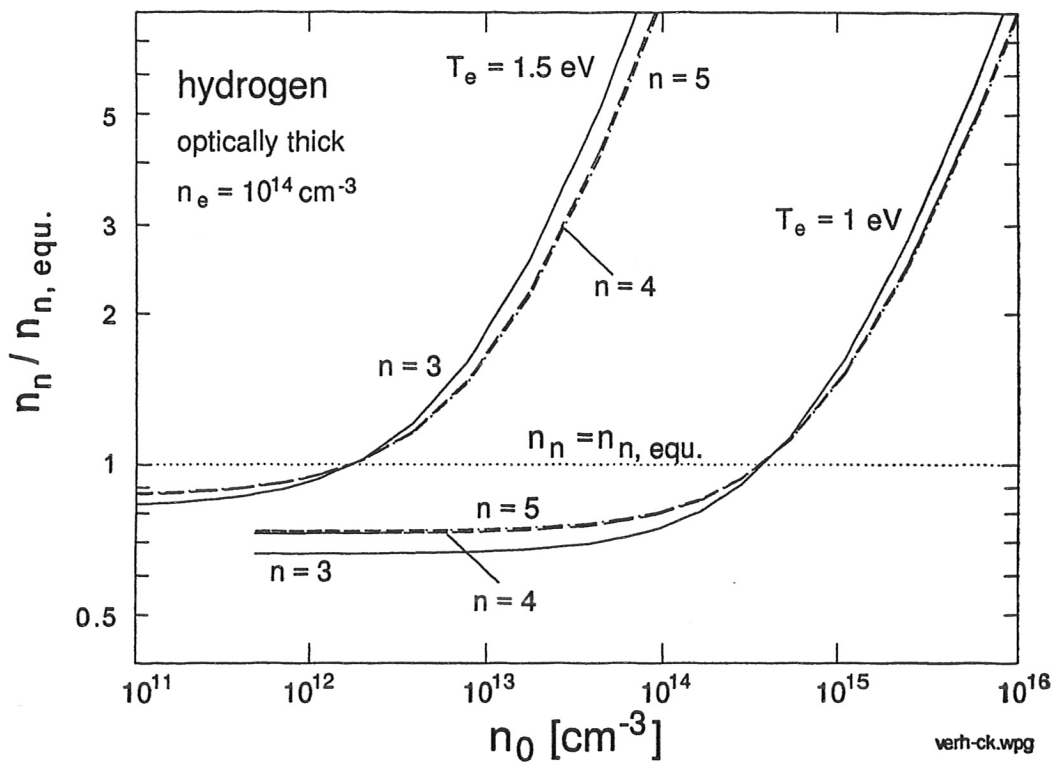


Fig.15: Population of excited hydrogen levels with respect to their equilibrium population as a function of n_0 . Optically thick case. The equilibrium neutral densities are $4.08 \cdot 10^{12} \text{ cm}^{-3}$ for 1.5 eV and $5.75 \cdot 10^{14} \text{ cm}^{-3}$ for 1 eV.

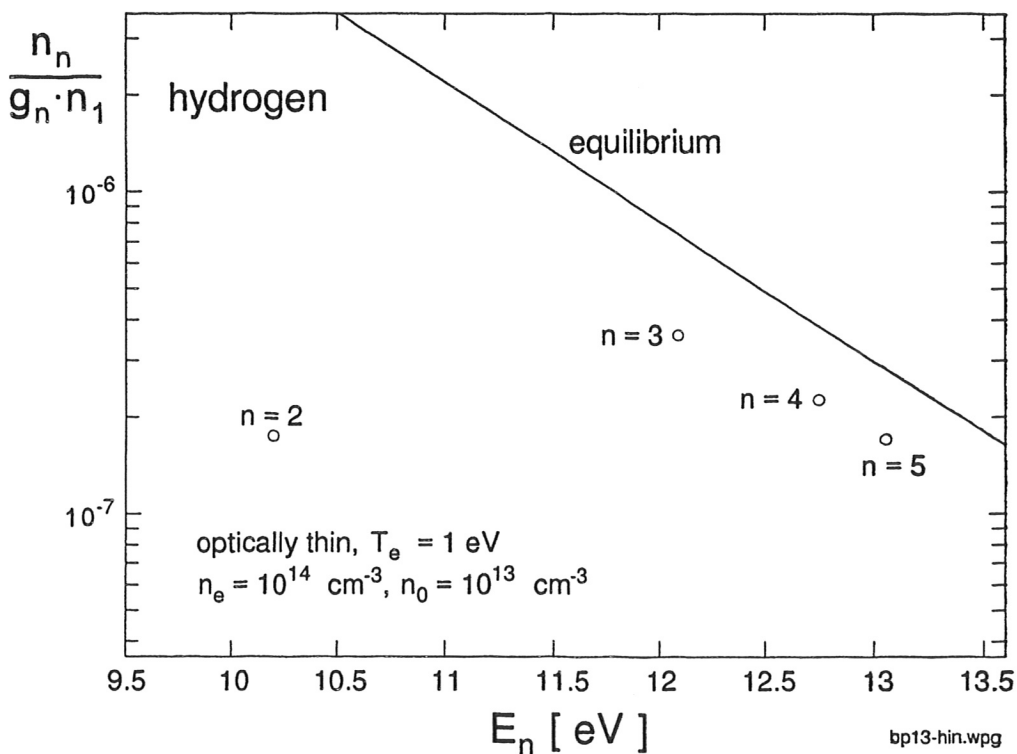


Fig.16: Boltzmann plot for 1 eV, optically thin case and a neutral density of 10^{13} cm^{-3} .